AGU PUBLICATIONS

Geophysical Research Letters

RESEARCH LETTER
10.1002/2015GL065999

Key Points:
- Holocene sea surface radiocarbon record was generated from NE Atlantic corals
- Sea surface hydrological changes occurred at 3.4, 2.7, 1.7, and 1.2 kyr B.P.
- Collapses in coral ecosystems in response to sea surface hydrological changes

Supporting Information:
- Texts S1–S3 and Tables S1–S3
- Table S1
- Table S2
- Table S3

Correspondence to:
M. Douarin,
melanie.douarin@univ-nantes.fr

Citation:
Douarin, M., M. Elliot, S. R. Noble, S. G. Moreton, D. Long, D. Sinclair, L.-A. Henry, and J. M. Roberts (2015), North Atlantic ecosystem sensitivity to Holocene shifts in Meridional Overturning Circulation, *Geophys. Res. Lett.*, *42*, doi:10.1002/2015GL065999.

Received 31 AUG 2015
Accepted 16 OCT 2015
Accepted article online 21 OCT 2015

North Atlantic ecosystem sensitivity to Holocene shifts in Meridional Overturning Circulation

Mélanie Douarin[1,2], Mary Elliot[1,2], Stephen R. Noble[3], Steven G. Moreton[4], David Long[5], Daniel Sinclair[6], Lea-Anne Henry[7], and J. Murray Roberts[7,8,9]

[1]Grant Institute of Earth Science, School of Geosciences, University of Edinburgh, Edinburgh, UK, [2]Laboratoire de Planétologie/Géodynamique, UMR-CNRS 6112, Université de Nantes, Nantes, France, [3]NERC Isotope Geosciences Laboratory, British Geological Survey, Nottingham, UK, [4]NERC Radiocarbon Facility (Environment), Scottish Enterprise Technology Park, Glasgow, UK, [5]British Geological Survey, Edinburgh, UK, [6]School of Geography Environment and Earth Sciences, Victoria University of Wellington, Wellington, New Zealand, [7]Centre for Marine Biodiversity and Biotechnology, School of Life Sciences, Heriot-Watt University, Edinburgh, UK, [8]Scottish Association for Marine Science, Scottish Marine Institute, Oban, UK, [9]Center for Marine Science, University of North Carolina at Wilmington, Wilmington, North Carolina, USA

Abstract Rapid changes in North Atlantic climate over the last millennia were driven by coupled sea surface/atmospheric processes and rates of deep water formation. Holocene climate changes, however, remain poorly documented due to a lack of high-resolution paleoclimate records, and their impacts on marine ecosystems remain unknown. We present a 4500 year absolute-dated sea surface radiocarbon record from northeast Atlantic cold-water corals. In contrast to the current view that surface ocean changes occurred on millennial-scale cycles, our record shows more abrupt changes in surface circulation. Changes were centered at 3.4, 2.7, 1.7, and 1.2 kyr B.P. and associated with atmospheric reorganization. Solar irradiance may have influenced these anomalies but changes in North Atlantic deep water convection are likely to have amplified these signals. Critically, we provide the first evidence that these perturbations in Atlantic Meridional Overturning Circulation led to the decline of cold-water coral ecosystems from 1.2 to ~0.1 kyr B.P.

1. Introduction

The Atlantic Meridional Overturning Circulation (AMOC) results in the ocean-scale transport of warm saline surface water masses northward and deeper southward circulation of cooler, fresher waters [*Hansen and Østerhus*, 2000; *Read*, 2001]. The surface limb of the AMOC, the North Atlantic Current (NAC), loses much of its heat to the atmosphere on its way north, which helps regulate the climate over Europe [*Hall and Bryden*, 1982]. The NAC follows the boundary between the North Atlantic subpolar gyre (SPG) and the subtropical gyre (STG), and its density and flow are modulated by the SPG [*Hátún et al*., 2005]. During periods when the SPG is enhanced (elongated E-W with strong outgrowth into the eastern Atlantic), the NAC transports fresher and cooler waters [*Hátún et al*., 2005]. The strength of the SPG is assumed to be interconnected with the strength of the AMOC and production of cold dense Labrador Sea water, although the mechanisms connecting these remain unresolved [*Häkkinen*, 2001]. Since the density of the NAC is critical in the formation of deep waters [*Hansen and Østerhus*, 2000], which in turn affect climate through changes in heat flux, fluctuations in SPG dynamics are likely to be associated with changes in global climate.

Sediment cores from the subpolar North Atlantic record cyclic millennial-scale oscillations in the North Atlantic surface water composition associated with reduced deep water convection during Holocene climatic deteriorations [*Bond et al*., 2001; *Oppo et al*., 2003; *Thornalley et al*., 2009]. Consistent with modern mechanisms, these records showed that Holocene climatic anomalies are likely to be controlled by SPG dynamics [*Thornalley et al*., 2009]. Centennial to millenial time scale oscillations in sea surface hydrology during the Holocene thus seem primarily governed by changes in wind stress and/or freshwater input to the Labrador Sea and appear to have affected SPG circulation [*Bond et al*., 2001; *Thornalley et al*., 2009]. The periodicity and triggers of these abrupt climatic events remain elusive but likely involve changes in solar activity or internal oceanic forcing [*Bond et al*., 2001; *Sorrel et al*., 2012]. High-resolution and well-dated sea surface records of the Northeast Atlantic combined with ice core data, for instance, are critical to strengthen our understanding of coupled ocean-atmosphere changes as well as defining any potential external driver such as solar activity.

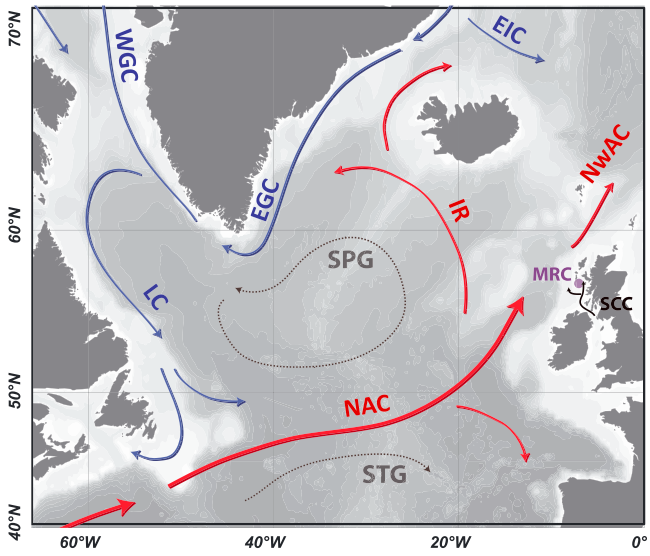

Figure 1. Location of the Mingulay Reef Complex (MRC; purple circle) and major surface circulation features of the North Atlantic showing how subpolar and subtropical (SPG and STG) waters meet, mix, and feed into the North Atlantic Current (NAC). Black arrows symbolized the Scottish Coastal Current (SCC). Red arrows show main branches of the warmer more saline North Atlantic Current (NAC), Norwegian Atlantic Current (NwAC), and Irminger Current (IR). Blue arrows show the main cooler fresher East Greenland Current (EGC), East Icelandic Current (EIC), West Greenland Current (WGC), and Labrador Current (LC). Note that an increase in the SPG will bring enhanced contribution of northern sourced waters to the NAC.

Holocene climatic deteriorations were probably severe enough to impact populations and entire ecosystems [*Alley et al.*, 2003], but evidence for ecosystem responses in the marine biome are lacking. The skeletons of cold-water scleractinian corals are excellent archives of past climate changes. Many species build substantial reef frameworks that support rich biological communities and commercially valuable fisheries resources [*Roberts et al.*, 2006]. Recent studies have hypothesized that North Atlantic abrupt hydrological changes have affected cold-water coral occurrence and growth over the Holocene [*Frank et al.*, 2009; *Douarin et al.*, 2013]. Thus, combining cold-water coral growth history reconstructions and records of sea surface hydrology will be of great value to understand how marine ecosystems responded to changes in their environments and to evaluate the consequences for fisheries and the global economy that depends on them. It is also critical that policy makers are equipped with accurate reconstructions of natural climate variability coupled with evidence for the sensitivity of marine ecosystems so that oceans can be managed in ways that enhance the resilience of these systems.

In this study, we used paired radiocarbon and U-series dates on cold-water corals to reconstruct atmosphere-ocean changes in the subpolar North Atlantic associated with abrupt Holocene climatic anomalies. Critically, we examined whether these anomalies impacted one of Earth's most complex and biologically diverse marine ecosystems, cold-water coral reefs [*Roberts et al.*, 2006].

2. Material and Methods

2.1. *Lophelia pertusa* Samples and Study Site

Seabed surface samples and downcore fragments of the coral *Lophelia pertusa* from the Mingulay Reef Complex were considered (56°50′N; 7°20′W; supporting information Text S1 and Table S1). These coral reefs are located in relatively shallow (121–162 m) waters on the Western British continental shelf [*Roberts et al.*, 2005] and are ideally suited to document episodes of enhanced vertical mixing and surface AMOC changes (Figure 1).

Presently, the deepest waters (>100 m) and the outer parts of the shelf of west Scotland are of Atlantic origin [*Inall et al.*, 2009]. The coral ecosystem off Mingulay is thus primary bathed by the NAC [*Dodds et al.*, 2007]. The Marine Reservoir Effect (MRE) of the NAC and derived branches averages about 400 years [*Stuiver et al.*, 1998]. However, the East Greenland Current (EGC) and Labrador Current (LC), for example, are major pathways of sea ice and freshwater input to the North Atlantic and are depleted in radiocarbon (MRE > 450–500 years) compared to the NAC [*Franke et al.*, 2008; *Eiríksson et al.*, 2011]. Enhanced SPG dynamics would favor the southward/eastward advection of these older waters to the NAC, raising the MRE in Mingulay [*Hátún et al.*, 2005]. The Scottish Coastal Current (SCC, originating from Atlantic and Irish Sea waters) is considered to have a very minor influence at our site [*Inall et al.*, 2009]. However, the contribution of this surface current that is enriched in radiocarbon relative to the NAC would tend to lower the MRE in our study site [*Ascough et al.*, 2009].

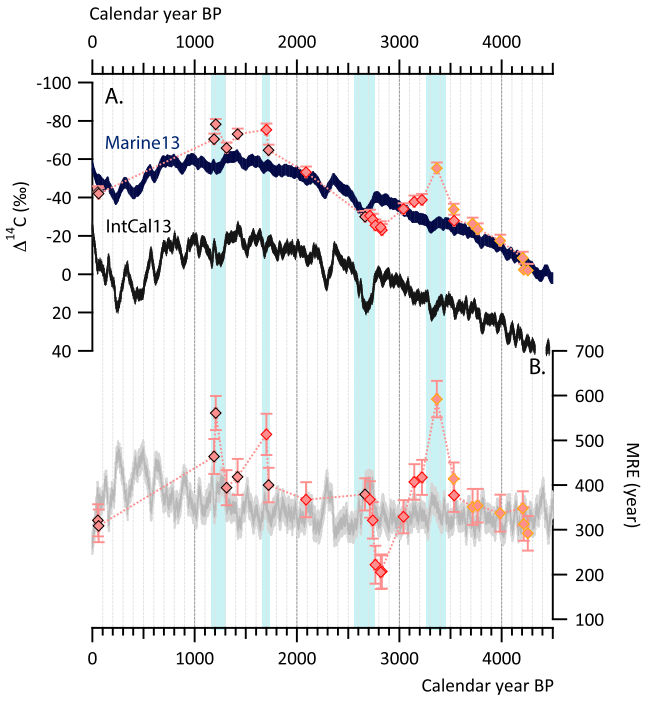

Figure 2. (a) $\Delta^{14}C$ reconstructed from Mingulay Reef Complex cold-water corals relative to the atmospheric (IntCal13) and modeled surface global ocean (Marine13) $\Delta^{14}C$ records [*Reimer*, 2013]. (b) MRE reconstructed from the same corals against the difference of the Marine13 and IntCal13 radiocarbon ages. Graphed are seabed surface samples (diamonds surrounded in black), samples from core 930 (diamonds surrounded in red), and samples from core 929 (diamonds surrounded in yellow). Error bars for $\Delta^{14}C$, MRE, and the U-series chronology are presented with 1 s uncertainties (note that the error bars may be smaller than the sample symbols used). The blue lines mark abrupt MRE increase.

2.2. Marine Radiocarbon Reconstructions

Radiocarbon was measured in U-series-dated coral fragments, previously used to generate a high-resolution record of reef growth [*Douarin et al.*, 2013, 2014]. The downcore U-series data published in *Douarin et al.* [2013] and new U-series data were recalculated using decay constants of *Cheng et al.* [2013] and uncertainties propagated using Monte Carlo techniques based on *McLean et al.* [2011] (supporting information Text S2 and Table S2).

$\Delta^{14}C$ of the water in which the coral grew was calculated from the U-series and radiocarbon ages of the corals following *Adkins and Boyle* [1997]. Coral $\Delta^{14}C$ was compared to the atmospheric and modeled surface global ocean $\Delta^{14}C$ curves to examine any regional deviation associated with climatic and oceanic variables [*Reimer*, 2013] (supporting information Text S3 and Table S3). The offset between the ^{14}C activity of the atmospheric and oceanic carbon reservoirs was calculated using the ResAge package [*Soulet*, 2015]. Also known as the Marine Reservoir Effect (MRE), it deviates spatially and temporally in response to the rate of atmosphere-ocean gas exchange (e.g., caused by wind stress and sea ice cover) and/or lateral advection [*Heier-Nielsen et al.*, 1995; *Tisnérat-Laborde et al.*, 2010]. The reconstructed MRE is therefore inferred to represent past oceanic and atmospheric changes associated with Holocene climatic anomalies. This high-resolution MRE record was also compared to the growth history of Mingulay reefs [*Douarin et al.*, 2013] to determine if abrupt climate changes impacted this cold-water coral reef ecosystem.

3. Results

The reconstructed $\Delta^{14}C$ values for the Mingulay corals closely match the modeled surface global ocean $\Delta^{14}C$ curves between 4.3–3.5, 2.7–1.8, and at 0.055 kyr B.P. (Figure 2a). The good agreement between the corresponding reconstructed MRE (290–410 years; Figure 2b) and the age difference between the modeled surface global ocean (Marine13) curve and the atmospheric radiocarbon curve (IntCal13) for these three periods confirm the strong influence of Atlantic origin waters (NAC) at Mingulay [*Dodds et al.*, 2007].

The first abrupt offset of the $\Delta^{14}C$ values for corals occurred between 3.5 and 3.4 kyr B.P. The corresponding MRE shifted from 414 ± 36 to 592 ± 41 years in just 100 years. MRE values steadily decrease until 2.8 kyr B.P. to 205 ± 37 years, followed by an abrupt increase over 100 years to 379 ± 36 years at 2.7 kyr B.P. The reconstructed $\Delta^{14}C$ values for corals exhibit two final deviations from IntCal13 and Marine13 at 1.7 and 1.2 kyr B.P., with MRE's of 513 ± 46 years and 561 ± 37 years, respectively (Figure 2b).

Atmospheric $\Delta^{14}C$ pulses (IntCal13), which are also seen in the modeled surface global ocean curve (Marine13), occurred synchronously with rather depleted $\Delta^{14}C$ for corals at 3.4, 1.7, and 1.2 kyr B.P. [*Reimer*, 2013] (Figure 2a). The abrupt return to Marine13-like $\Delta^{14}C$ seen at 2.7 kyr B.P. also matches a sharp atmospheric

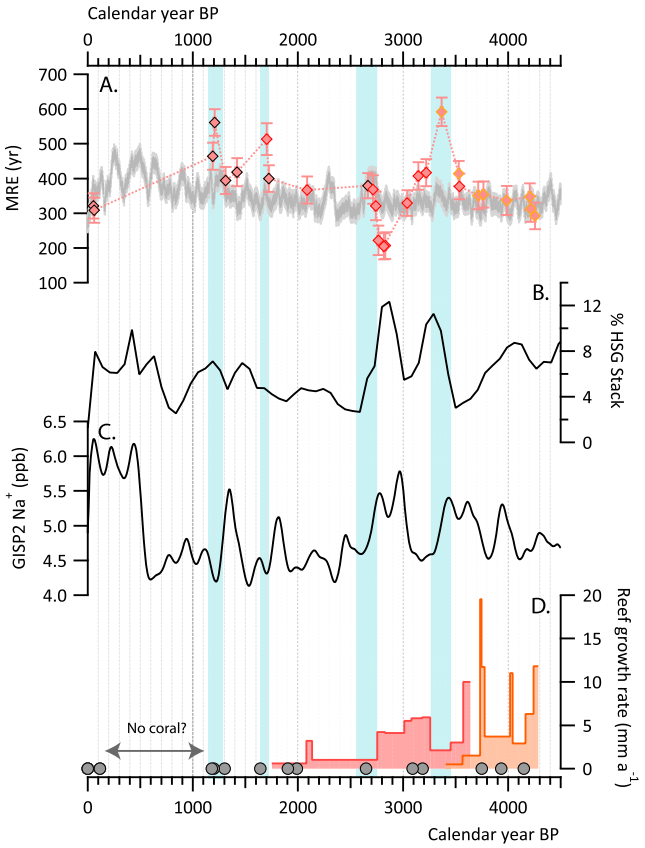

Figure 3. (a) MRE reconstructed from Mingulay Reef Complex cold-water corals against the difference of the Marine13 and IntCal13 radiocarbon ages [*Reimer*, 2013]. MRE symbols are as for Figure 2: seabed surface samples (diamonds surrounded in black), samples from core 930 (diamonds surrounded in red), and samples from core 929 (diamonds surrounded in yellow). (b) Hematite-strained grains (%) from North Atlantic cores stack as a proxy of advections of cooler, ice-bearing surface waters eastward from the Labrador Sea and southward from the Nordic Seas [*Bond et al.*, 2001]. (c) Greenland Ice Sheet Project 2 sea-salt sodium as a proxy of westerly winds (two-pass low-pass filter with a cutoff frequency at 1/200 Hz) [*O'Brien et al.*, 1995]. (d) Reef growth rates estimated from downcore +56-08/930VE (pink) and downcore +56-08/929VE (orange) U-series chonologies; grey dots indicate ages for seabed surface *Lophelia* dated by radiocarbon and/or U-series [*Douarin et al.*, 2013]. The blue lines indicate abrupt MRE increase. Error bars are presented with 1 s uncertainties and may be smaller than the sample symbols.

$\Delta^{14}C$ pulse (IntCal13). This inverse correlation between atmospheric and coral $\Delta^{14}C$ suggests that coral radiocarbon responded to oceanic and climate (sea ice extent and atmospheric) variables rather than a lagged response to changing atmospheric ^{14}C concentrations.

4. Discussion

4. 1. Origin of Holocene Sea Surface Radiocarbon Variability

The low and/or declining ^{14}C events in the Mingulay corals at 3.4, 2.7, 1.7, and 1.2 kyr B.P. are consistent with southward and eastward advection of ^{14}C-depleted Arctic origin waters during periods of enhanced SPG circulation [*Ascough et al.*, 2009; *Eiríksson et al.*, 2011]. This is supported by the correlation between these events and peaks in hematite-stained grains in North Atlantic sediment cores (which are an independent proxy for the influx of cooler, ice-bearing surface waters from the Labrador and Nordic Seas; Figures 3a and 3b) [*Bond et al.*, 2001]. It is notable that while continuous sediment records have previously demonstrated that these SPG dynamics occurred over millennial timescales [*Bond et al.*, 2001; *Thornalley et al.*, 2009], our high-resolution $\Delta^{14}C$ reconstruction from Mingulay reveals for the first time that even shorter and more abrupt centennial-scale episodes of enhanced SPG water influence occurred during the late Holocene (Figure 3a). This highlights that sediment core records may be biased by factors such as bioturbation and low sedimentation rates that limit our ability to obtain records with less than millennial resolution. In addition, age models and the precise timing of the abrupt hydrological changes documented by such records relying on radiocarbon analyses can also be biased by variations in reservoir ages. Thus, the temporal weakness of the available marine record may well explain the temporal mismatch between available records. This, highlighting the need to provide more absolute dated and highly resolved sea surface records. The abrupt changes in variations in SPG dynamics recorded in this study would potentially have modified the density of the northward flowing NAC and reduced the meridional heat flux thus affected climate over Europe (Figure 3a).

What caused the SPG circulation to increase remains uncertain, but one possibility is that enhanced westerlies over the North Atlantic increased wind stress, driving enhanced gyre circulation [*Thornalley et al.*, 2009]. Low/declining ^{14}C events in the corals are preceded by periods of elevated Na^+ in Greenland Ice Sheet Project 2 (GISP2) ice core which are interpreted as sea salt transported by strengthened westerly winds [*O'Brien et al.*, 1995; *Mayewski et al.*, 2004; *Jackson et al.*, 2005] (Figures 3a and 3c). Thus, enhanced SPG

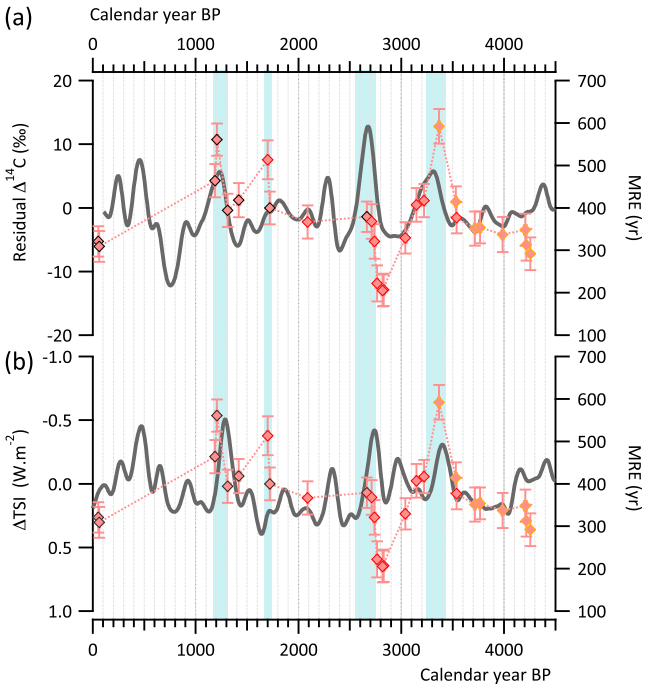

Figure 4. MRE reconstructed from Mingulay Reef Complex cold-water corals relative to (a) the Residual atmospheric $\Delta^{14}C$ curve [*Reimer et al.*, 2004] and (b) the Δ total solar irradiance (two-pass low-pass filter with a cutoff frequency at 1/200 Hz) [*Steinhilber et al.*, 2009]. Uncertainties are presented by 1 s error bars and may be smaller than the sample symbols. The blue lines symbolized abrupt MRE increase.

circulation may have been caused by increased wind stress. We can only speculate as to the ultimate driver of these enhanced SPG events. Solar forcing is one possibility [*Stuiver and Braziunas*, 1993; *Bond et al.*, 2001; *Helama et al.*, 2010] as the low/declining ^{14}C events in the coral are synchronous with sharp centennial-scale troughs in total solar irradiance at 3.4, 2.8, 1.7 ka B.P. and 1.3 kyr B.P. [*Steinhilber et al.*, 2009] (Figures 4a and 4b). The mechanism is not clear, but solar forcing appears to play a role in Holocene climatic anomalies, an effect that is amplified by ocean/atmosphere feedbacks, possibly through reduction in North Atlantic deep water formation [*Stuiver and Braziunas*, 1993; *Bond et al.*, 2001; *Rind*, 2002; *Jongma et al.*, 2007]. Since the North Atlantic deep water convection is a major component of the transport and sequestration of heat and atmospheric ^{14}C to the deep sea [*Clark et al.*, 2002], a reduction in deep water formation could amplify climatic anomalies and would have also resulted in elevated atmospheric $\Delta^{14}C$ [*Stuiver and Braziunas*, 1993]. A correlation between the low/declining ^{14}C in the Mingulay coral and enhanced residual atmospheric $\Delta^{14}C$ values (Figures 4a and 4b) thus supports the prevailing concept that low solar irradiance plays a role in triggering enhanced SPG circulation.

The unusual enrichment in $\Delta^{14}C$ seen in the coral record at 2.8 kyr B.P. (Figure 3a) could be either interpreted as enhanced advection of radiocarbon-enriched water masses or enhanced gas exchange rates between the atmosphere and the surface mixing layers [*Ascough et al.*, 2009; *Tisnérat-Laborde et al.*, 2010; *Wanamaker et al.*, 2012]. We cannot at this stage easily reject either mechanism, although periods of climate change in the North Atlantic have been associated with strong connection between atmospheric and ocean circulation implying that enhanced rates of gas exchange are a plausible explanation [*O'Brien et al.*, 1995; *Thornalley et al.*, 2009; *Sorrel et al.*, 2012]. This episode is synchronous with strengthened westerly winds from Na^+ in GISP2 ice cores record. Enhanced wind stress could have contributed to homogenized the water column-inducing enriched $\Delta^{14}C$ values from corals (Figure 3c). However, enhanced and stronger influence of STG water (enriched $\Delta^{14}C$) to the NAC could also be seen as a mechanism that stabilizes AMOC [*Oppo et al.*, 2003; *Thornalley et al.*, 2009]. Thus, the strengthened SPG circulation reported in our record 3.4 ka B.P. ago would have in turn reduced deep water convection, such as that reported by *Oppo et al.* [2003]. The subsequent convective shutdown would have reduced the SPG circulation and favored the enhanced influence of STG waters to the North Atlantic, which would have been essential to restart deep convection and stabilize AMOC [*Thornalley et al.*, 2009]. Providing more absolute dated and highly resolved sea surface records that would be directly comparable with ice core records would constitute a stepping stone toward understanding coupled ocean-atmosphere climatic system.

4.2. Sensitivity of Marine Ecosystems

Cold-water corals construct complex three-dimensional reef framework habitats for thousands of animal species including commercially exploited fish and constitute a globally distributed but vulnerable ecosystem that needs to be conserved [*Roberts et al.*, 2006]. The sensitivities of these and other marine "ecosystem engineers"

to changes in their environments are poorly constrained. Shifts in the distribution of cold-water coral ecosystems over glacial/interglacial cycles and during the Holocene are typically attributed to changes in the physical and biological dynamics of their environments [*Frank et al*., 2011; *Douarin et al*., 2013; *Margolin et al*., 2013; *Thiagarajan et al*., 2013; *Henry et al*., 2014]. Biogeochemical cycles driving productivity in the North Atlantic are sensitive to perturbation of the AMOC and potentially impact marine ecosystem [*Schmittner*, 2005]. For example, past changes in food supply have had significant control on coral occurrence and reef growth over thousands of years [*Eisele et al*., 2011; *Frank et al*., 2011; *Thiagarajan et al*., 2013; *Hebbeln et al*., 2014]. Other parameters affected by changes to the AMOC include larval supply, temperature, and dissolved oxygen and carbonate ion concentration, and these can also exert strong control in these ecosystems [*Dodds et al*., 2007; *Davies et al*., 2008; *Thiagarajan et al*., 2013; *Douarin et al*., 2014; *Henry et al*., 2014]. Rapid changes in AMOC dynamics during the Holocene would therefore be expected to impact cold-water coral ecosystems, but to date proxy records of circulation changes have lacked the temporal resolution to study these effects.

In Figure 3a and 3d the growth history of Mingulay Reef Complex was compared with the reconstructed MRE. This reveals that the sharp increase in MRE between 3.4 and 3.3 kyr B.P. was closely correlated with reduced reef growth, suggesting that the abrupt increase in SPG circulation initially destabilized the ecosystem. After 3.3 kyr B.P. a progressive return of MRE values to close and even below that of the mean global ocean seems to have promoted reef growth and ecosystem recovery. The next sharp increase in the MRE from 2.8 kyr B.P. to 2.7 kyr B.P. marks another reduction in coral growth. The final hydrological shifts at 1.7 kyr B.P. and 1.2 kyr B.P. also appear to have been detrimental and triggered a severe decline in this already apparently weakened ecosystem. It is noteworthy that none of the 60 dated corals came from the interval 1.2–0.055 kyr B.P. implying that this degraded ecosystem state persisted for a thousand years.

Numerous paleoenvironmental records indicate an abrupt climatic anomaly during the Little Ice Age (LIA) at ~ 0.7–0.15 kyr B.P. [*Wanner et al*., 2008]. This period was characterized by an enhanced Arctic water influence to the subpolar Atlantic [*Wanamaker et al*., 2012] and is thus comparable to those we have documented at 3.4, 2.7, 1.7, and 1.2 kyr B.P. These conditions appear to have been unsuitable for coral reef growth in the NE Atlantic [*Douarin et al*., 2013] and may explain the extended period of ecosystem decline at Mingulay. The reduced supply of NAC-derived Atlantic water to Mingulay during the LIA may also have limited inflow of coral larvae from deeper or more southerly coral sites [*Henry et al*., 2014] preventing recolonization until the circulation of Arctic water reduced at 0.055 kyr B.P. [*Wanamaker et al*., 2012].

This study reveals the sensitivity of marine ecosystems to sea surface hydrological changes associated with Holocene abrupt climatic anomalies. The known vulnerability of fragile cold-water coral reef ecosystems to impacts of commercial fishing combined [*Roberts et al*., 2006] with this evidence of their sensitivity to abrupt climatic and oceanic change underscore the importance of implementing well-connected and internationally managed networks of marine protected areas that can enhance ecosystem resilience in areas destabilized by human activities and exposed to the rapid progression of ocean warming and acidification [*Hennige et al*., 2015].

5. Conclusion

This study presents a new high-resolution absolute-dated Holocene sea surface radiocarbon record from scleractinian cold-water corals in the northeast Atlantic. Abrupt centennial-scale episodes of coupled atmosphere-ocean reorganization were reported at 3.4 ka B.P., 2.7–2.8 ka B.P., 1.7 ka B.P., and 1.2 ka B.P. The unprecedented centennial resolution of this record demonstrate that sea surface hydrology changes associated with Holocene abrupt climatic anomalies happened much more abruptly than previously thought. The parallel with coral reef growth rate estimates shows that successive abrupt collapses in cold-water coral occurred in response to the coupled atmosphere-ocean reorganization and led to a pervasive thousand-year long demise of the ecosystem. The study highlights the sensitivity and speed with which deep water marine ecosystems respond to sea surface hydrological changes associated with abrupt climatic change.

Acknowledgments

M.D. acknowledges support from the British Geological Survey (BGS) and the Scottish Alliance for Geoscience, Environment and Society (SAGES). The authors are grateful for the support of NERC for access to facilities on the RRS *James Cook*, for the BGS for coring equipment and core processing facilities, and for the Scottish Association for Marine Sciences (SAMS) for hosting M.D. during the early phase of this project. J.M.R. acknowledges support from NERC through the UK Ocean Acidification programme and subsequent awards (NE/H017305/1 and NE/J021121/1). We thank Nicholas Odling from the University of Edinburgh for XRD screening, Neil Boulton of NIGL for assistance with U-series sample preparation, and Callum Murray for sample preparation for ^{14}C analyses and staff at the SUERC AMS Laboratory for the ^{14}C measurement. S.R.N. and D.L. publish with permission of the Executive Director, British Geological Survey (NERC). Noah McLean is thanked for the use of his U-series uncertainty propagation algorithms. We thank Kim Cobb and the anonymous reviewers for their constructive comments. Data are included as two tables (Tables S2 and S3) in a supporting information file; any additional data may be obtained from M.D. (melanie.douarin@univ-nantes.fr).

References

Adkins, J. F., and E. A. Boyle (1997), Changing atmospheric $\Delta^{14}C$ and the record of deep water paleoventilation ages, *Paleoceanography*, *12*, 337–344, doi:10.1029/97PA00379.

Alley, R. B., et al. (2003), Abrupt climate change, *Science*, *299*(5615), 2005–2010, doi:10.1126/science.1081056.

Ascough, P. L., G. T. Cook, and A. J. Dugmore (2009), North Atlantic marine ^{14}C reservoir effects: Implications for late-Holocene chronological studies, *Quat. Geochronol.*, *4*(3), 171–180, doi:10.1016/j.quageo.2008.12.002.

Bond, G., B. Kromer, J. Beer, R. Muscheler, M. N. Evans, W. Showers, S. Hoffmann, R. Lotti-Bond, I. Hajdas, and G. Bonani (2001), Persistent solar influence on North Atlantic climate during the Holocene, *Science*, *294*(5549), 2130–2136, doi:10.1126/science.1065680.

Cheng, H., et al. (2013), Improvements in ^{230}Th dating, ^{230}Th and ^{234}U half-life values, and U-Th isotopic measurements by multi-collector inductively coupled plasma mass spectrometry, *Earth Planet. Sci. Lett.*, *371-372*, 82–91, doi:10.1016/j.epsl.2013.04.006.

Clark, P. U., N. G. Pisias, T. F. Stocker, and A. J. Weaver (2002), The role of the thermohaline circulation in abrupt climate change, *Nature*, *415*, 863–869, doi:10.1038/415863a.

Davies, A. J., M. Wisshak, J. C. Orr, and J. Murray Roberts (2008), Predicting suitable habitat for the cold-water coral Lophelia pertusa (Scleractinia), *Deep Sea Res., Part I*, *55*(8), 1048–1062, doi:10.1016/j.dsr.2008.04.010.

Dodds, L. A., J. M. Roberts, A. C. Taylor, and F. Marubini (2007), Metabolic tolerance of the cold-water coral *Lophelia pertusa* (Scleractinia) to temperature and dissolved oxygen change, *J. Exp. Mar. Biol. Ecol.*, *349*, 205–214, doi:10.1016/j.jembe.2007.05.013.

Douarin, M., M. Elliot, S. R. Noble, D. Sinclair, L.-A. Henry, D. Long, S. G. Moreton, and J. M. Roberts (2013), Growth of north-east Atlantic cold-water coral reefs and mounds during the Holocene: A high resolution U-series and ^{14}C chronology, *Earth Planet. Sci. Lett.*, *375*, 176–187.

Douarin, M., D. J. Sinclair, M. Elliot, L.-A. Henry, D. Long, F. Mitchison, and J. M. Roberts (2014), Changes in fossil assemblage in sediment cores from Mingulay Reef Complex (NE Atlantic): Implications for coral reef build-up, *Deep Sea Res., Part II*, *99*, 286–296.

Eiríksson, J., K. L. Knudsen, G. Larsen, J. Olsen, J. Heinemeier, H. B. Bartels-Jónsdóttir, H. Jiang, L. Ran, and L. A. Símonarson (2011), Coupling of palaeoceanographic shifts and changes in marine reservoir ages off North Iceland through the last millennium, *Palaeogeogr. Palaeoclimatol. Palaeoecol.*, *302*, 95–108, doi:10.1016/j.palaeo.2010.06.002.

Eisele, M., N. Frank, C. Wienberg, D. Hebbeln, M. López Correa, E. Douville, and A. Freiwald (2011), Productivity controlled cold-water coral growth periods during the last glacial off Mauritania, *Mar. Geol.*, *280*(1–4), 143–149, doi:10.1016/j.margeo.2010.12.007.

Frank, N., et al. (2009), The Holocene occurrence of cold water corals in the NE Atlantic: Implications for coral carbonate mound evolution, *Mar. Geol.*, *266*(1–4), 129–142.

Frank, N., et al. (2011), Northeastern Atlantic cold-water coral reefs and climate, *Geology*, *8*, 743–746, doi:10.1130/G31825.1.

Franke, J., A. Paul, and M. Schulz (2008), Modeling variations of marine reservoir ages during the last 45 000 years, *Clim. Past Discuss.*, *4*, 81–110, doi:10.5194/cpd-4-81-2008.

Häkkinen, S. (2001), Variability in sea surface height: A qualitative measure for the meridional overturning in the North Atlantic, *J. Geophys. Res.*, *106*, 13,837–13,848, doi:10.1029/1999JC000155.

Hall, M. M., and H. L. Bryden (1982), Direct estimates and mechanisms of ocean heat transport, *Deep Sea Res., Part A.*, *29*, 339–359, doi:10.1016/0198-0149(82)90099-1.

Hansen, B., and S. Østerhus (2000), North Atlantic-Nordic Seas exchanges, *Prog. Oceanogr.*, *45*, 109–208, doi:10.1016/S0079-6611(99)00052-X.

Hátún, H., A. B. Sandø, H. Drange, B. Hansen, and H. Valdimarsson (2005), Influence of the Atlantic subpolar gyre on the thermohaline circulation, *Science*, *309*(5742), 1841–4, doi:10.1126/science.1114777.

Hebbeln, D., et al. (2014), Environmental forcing of the Campeche cold-water coral province, southern Gulf of Mexico, *Biogeosciences*, *11*(7), 1799–1815, doi:10.5194/bg-11-1799-2014.

Heier-Nielsen, S., J. Heinemeier, H. L. Nielsen, and N. Rud (1995), Recent reservoir ages for Danish fjords and marine waters, *Radiocarbon*, *37*, 875–882.

Helama, S., M. M. Fauria, K. Mielikainen, M. Timonen, and M. Eronen (2010), Sub-Milankovitch solar forcing of past climates: Mid and late Holocene perspectives, *Geol. Soc. Am. Bull.*, *122*, 1981–1988, doi:10.1130/B30088.1.

Hennige, S. J., L. C. Wicks, N. A. Kamenos, G. Perna, H. S. Findlay, and J. M. Roberts (2015), Hidden impacts of ocean acidification to live and dead coral framework, *Proc. R. Soc. B*, doi:10.1098/rspb.2015.0990.

Henry, L.-A., et al. (2014), Global ocean conveyor lowers extinction risk in the deep sea, *Deep Sea Res., Part I*, *88*, 8–16.

Inall, M., P. Gillibrand, C. Griffiths, N. MacDougal, and K. Blackwell (2009), On the oceanographic variability of the North-West European Shelf to the West of Scotland, *J. Mar. Syst.*, *77*(3), 210–226.

Jackson, M. G., N. Oskarsson, R. G. Trønnes, J. F. McManus, D. W. Oppo, K. Grönvold, S. R. Hart, and J. P. Sachs (2005), Holocene loess deposition in Iceland: Evidence for millennial-scale atmosphere-ocean coupling in the North Atlantic, *Geology*, *33*, 509–512, doi:10.1130/G21489.1.

Jongma, J. I., M. Prange, H. Renssen, and M. Schulz (2007), Amplification of Holocene multicentennial climate forcing by mode transitions in North Atlantic overturning circulation, *Geophys. Res. Lett.*, *34*, L15706, doi:10.1029/2007GL030642.

Margolin, A. R., L. F. Robinson, A. Burke, R. G. Waller, K. M. Scanlon, M. L. Roberts, M. E. Auro, and T. van de Flierdt (2013), Temporal and spatial distributions of cold-water corals in the Drake Passage: Insights from the last 35,000 years, *Deep Sea Res., Part II*, *99*, 237–248, doi:10.1016/j.dsr2.2013.06.008.

Mayewski, P. A., et al. (2004), Holocene climate variability, *Quat. Res.*, *62*(3), 243–255, doi:10.1016/j.yqres.2004.07.001.

McLean, N. M., J. F. Bowring, and S. A. Bowring (2011), An algorithm for U-Pb isotope dilution data reduction and uncertainty propagation, *Geochem. Geophys. Geosyst.*, *12*, Q0AA18, doi:10.1029/2010GC003478.

O'Brien, S. R., P. A. Mayewski, L. D. Meeker, D. A. Meese, M. S. Twickler, and S. I. Whitlow (1995), Complexity of Holocene Climate as reconstructed from a Greenland Ice Core, *Science*, *270*, 1962–1964, doi:10.1126/science.270.5244.1962.

Oppo, D. W., J. F. McManus, and J. L. Cullen (2003), Palaeo-oceanography: Deepwater variability in the Holocene epoch, *Nature*, *422*, 277, doi:10.1038/422277b.

Read, J. F. (2001), CONVEX-91: Water masses and circulation of the Northeast Atlantic subpolar gyre, *Prog. Oceanogr.*, *48*, 461–510.

Reimer, P. (2013), IntCal13 and Marine13 radiocarbon age calibration curves 0–50,000 years cal BP, *Radiocarbon*, *55*, 1869–1887, doi:10.2458/azu_js_rc.55.16947.

Reimer, P. J., et al. (2004), IntCal04 terrestrial radiocarbon age calibration, 0–26 cal kyr BP, *Radiocarbon*, *46*(3), 1029–1058.

Rind, D. (2002), The Sun's role in climate variations, *Science*, *296*, 673–677, doi:10.1126/science.1069562.

Roberts, J. M., C. J. Brown, D. Long, and C. R. Bates (2005), Acoustic mapping using a multibeam echosounder reveals cold-water coral reefs and surrounding habitats, *Coral Reefs*, *24*(4), 654–669, doi:10.1007/s00338-005-0049-6.

Roberts, J. M., A. J. Wheeler, and A. Freiwald (2006), Reefs of the deep: The biology and geology of cold-water coral ecosystems, *Science*, *312*(5773), 543–7, doi:10.1126/science.1119861.

Schmittner, A. (2005), Decline of the marine ecosystem caused by a reduction in the Atlantic overturning circulation, *Nature*, *434*, 628–633, doi:10.1038/nature03476.

Sorrel, P., M. Debret, I. Billeaud, S. L. Jaccard, J. F. McManus, and B. Tessier (2012), Persistent non-solar forcing of Holocene storm dynamics in coastal sedimentary archives, *Nat. Geosci.*, *5*, 892–896, doi:10.1038/ngeo1619.

Soulet, G. (2015), Methods and codes for reservoir–atmosphere ^{14}C age offset calculations, *Quat. Geochronol.*, *29*, 97–103, doi:10.1016/j.quageo.2015.05.023.

Steinhilber, F., J. Beer, and C. Fröhlich (2009), Total solar irradiance during the Holocene, *Geophys. Res. Lett.*, *36*, L19704, doi:10.1029/2009GL040142.

Stuiver, M., and T. F. Braziunas (1993), Sun, ocean, climate and atmospheric $^{14}CO_2$: An evaluation of causal and spectral relationships, *Holocene*, *3*, 289–305, doi:10.1177/095968369300300401.

Stuiver, M., P. J. Reimer, and T. F. Braziunas (1998), High-precision radiocarbon age calibration for terrestrial and marine samples, *Radiocarbon*, *40*, 1127–1151, doi:10.2458/azu_js_rc.v40i3.3786.

Thiagarajan, N., D. Gerlach, M. L. Roberts, A. Burke, A. McNichol, W. J. Jenkins, A. V. Subhas, R. E. Thresher, and J. F. Adkins (2013), Movement of deep-sea coral populations on climatic timescales, *Paleoceanography*, *28*, 227–236, doi:10.1002/palo.20023.

Thornalley, D. J. R., H. Elderfield, and I. N. McCave (2009), Holocene oscillations in temperature and salinity of the surface subpolar North Atlantic, *Nature*, *457*(7230), 711–4, doi:10.1038/nature07717.

Tisnérat-Laborde, N., M. Paterne, B. Métivier, M. Arnold, P. Yiou, D. Blamart, and S. Raynaud (2010), Variability of the northeast Atlantic sea surface $\Delta^{14}C$ and marine reservoir age and the North Atlantic Oscillation (NAO), *Quat. Sci. Rev.*, *29*(19–20), 2633–2646, doi:10.1016/j.quascirev.2010.06.013.

Wanamaker, A. D., P. G. Butler, J. D. Scourse, J. Heinemeier, J. Eiríksson, K. L. Knudsen, and C. A. Richardson (2012), Surface changes in the North Atlantic Meridional Overturning Circulation during the last millennium, *Nat. Commun.*, *3*, 899, doi:10.1038/ncomms1901.

Wanner, H., et al. (2008), Mid- to Late Holocene climate change: An overview, *Quat. Sci. Rev.*, *27*(19–20), 1791–1828, doi:10.1016/j.quascirev.2008.06.013.

Table 1

Sample name	Sample collector	Collection date	Location	Latitude N/S	Longitude E/W	Water depth (m)
Seabed surface						
1151	Video-grab	15/05/05	Mingulay 1	56°49'08"	-7°23'36"	121
HWU20110609/002A	Video-grab	09/06/11	Mingulay 1	56°48'59"	-7°23'36"	162
Top core 56-08/928	Vibro-corer	26/09/07	Mingulay 5 N	56°47'08"	-7°25'48"	136
D340B/1496a	Video-grab	02/07/09	Mingulay 1	56°49'21"	-7°23'44"	125
1157	Video-grab	15/05/05	Mingulay 5 N	56°47'15"	-7°24'27"	122
HWU20110608/012A	Video-grab	08/06/11	Mingulay 1	56°49'33"	-7°23'52"	162
HWU20110707/008A	Video-grab	07/07/11	Mingulay 1	56°49'42"	-7°23'50"	134
Core +56-08/929VE						
929 A/4 3-9 cm	Vibro-corer	04/10/2007	Mingulay 1	56°49'19"	-7°23'27"	127
929 A/4 12-17 cm	Vibro-corer	04/10/2007	Mingulay 1	56°49'19"	-7°23'27"	127
929 A/4 90-91cm	Vibro-corer	04/10/2007	Mingulay 1	56°49'19"	-7°23'27"	127
929 B/4 106-108 cm	Vibro-corer	04/10/2007	Mingulay 1	56°49'19"	-7°23'27"	127
929 B/4 188-189 cm	Vibro-corer	04/10/2007	Mingulay 1	56°49'19"	-7°23'27"	127
929 C/4 284-290 cm	Vibro-corer	04/10/2007	Mingulay 1	56°49'19"	-7°23'27"	127
929 D/4 310-312 cm	Vibro-corer	04/10/2007	Mingulay 1	56°49'19"	-7°23'27"	127
929 D/4 349-353 cm	Vibro-corer	04/10/2007	Mingulay 1	56°49'19"	-7°23'27"	127
Core +56-08/930VE						
930 A/6 4-6 cm	Vibro-corer	04/10/2007	Mingulay 1	56°49'20"	-7°23'47"	134
930 A/6 42-45 cm	Vibro-corer	04/10/2007	Mingulay 1	56°49'20"	-7°23'47"	134
930 B/6 107-110 cm	Vibro-corer	04/10/2007	Mingulay 1	56°49'20"	-7°23'47"	134
930 B/6 134-137 cm	Vibro-corer	04/10/2007	Mingulay 1	56°49'20"	-7°23'47"	134
930 B/6 142-146 cm	Vibro-corer	04/10/2007	Mingulay 1	56°49'20"	-7°23'47"	134
930 C/6 251-254 cm	Vibro-corer	04/10/2007	Mingulay 1	56°49'20"	-7°23'47"	134
930 D/6 312-314 cm	Vibro-corer	04/10/2007	Mingulay 1	56°49'20"	-7°23'47"	134
930 D/6 356-358 cm	Vibro-corer	04/10/2007	Mingulay 1	56°49'20"	-7°23'47"	134
930 D/6 377-379 cm	Vibro-corer	04/10/2007	Mingulay 1	56°49'20"	-7°23'47"	134
930 D/6 388-392 cm	Vibro-corer	04/10/2007	Mingulay 1	56°49'20"	-7°23'47"	134
930 E/6 438-440 cm	Vibro-corer	04/10/2007	Mingulay 1	56°49'20"	-7°23'47"	134

Table 2

Sample Name	Lab number	[a]Depth (cm)	^{238}U ppm	±2s (abs)	^{232}Th ppb	±2s (abs)	$^{230}Th/^{232}Th_{AR}$	±2s (%)	$^{230}Th/^{238}U_{AR}$	±2s (%)	$^{234}U/^{238}U_{AR}$	±2s (%)	$\rho_{(08-48)}$	[b]Date uncorr (ka)	±2s (abs)	[c]Date corr (ka)	Date corr (ka BP_{1950})	±2s (abs)	$\delta^{234}U_i$	±2s (‰)
929 A/4 3-9 cm	**36/8**	**6.0±3.0**	3.354	±0.004	0.1409	±0.0006	2573.5	±0.43	0.03540	±0.49	1.1432	±0.11	0.0003	3.441	0.016	**3.428**	**3.367**	**0.018**	144.6	1.1
929 A/4 12-17 cm	**24/1**	**14.5±2.5**	3.747	±0.009	0.1361	±0.0004	3122.0	±0.37	0.03716	±0.37	1.1462	±0.25	0.0001	3.603	0.015	**3.591**	**3.530**	**0.016**	147.7	2.5
929 A/4 90-91cm	**39/9**	**90.5±0.5**	3.047	±0.003	0.1250	±0.0002	2938.1	±0.16	0.03947	±0.32	1.1438	±0.11	0.0005	3.839	0.011	**3.826**	**3.765**	**0.013**	145.4	1.1
929 B/4 106-108 cm	**36/9**	**107.0±1.0**	3.098	±0.003	0.1458	±0.0006	2526.9	±0.43	0.03893	±0.49	1.1428	±0.11	0.0004	3.792	0.017	**3.777**	**3.716**	**0.019**	144.4	1.1
929 B/4 188-189 cm	**35/3**	**188.5±0.5**	3.123	±0.004	0.2477	±0.0004	1605.1	±0.14	0.04158	±0.43	1.1405	±0.12	0.0011	4.072	0.011	**4.047**	**3.986**	**0.018**	142.1	1.2
929 C/4 284-290 cm	**35/1**	**287.0±3.0**	2.723	±0.003	0.1465	±0.0003	2498.2	±0.19	0.04400	±0.35	1.1431	±0.11	0.0006	4.294	0.012	**4.277**	**4.216**	**0.016**	144.8	1.1
929 D/4 310-312 cm	**36/10**	**311.0±1.0**	3.076	±0.003	0.2044	±0.0008	2018.7	±0.44	0.04387	±0.53	1.1422	±0.11	0.0007	4.288	0.020	**4.268**	**4.207**	**0.023**	144.0	1.1
929 D/4 349-353 cm	**35/6**	**351.0±2.0**	2.980	±0.003	0.3327	±0.0005	1218.8	±0.15	0.04437	±0.54	1.1422	±0.11	0.0018	4.352	0.011	**4.317**	**4.256**	**0.024**	143.9	1.1
930 A/6 4-6 cm	**35/8**	**5.0±1.0**	3.473	±0.004	0.4740	±0.0011	417.6	±0.24	0.01829	±1.50	1.1403	±0.11	0.0026	1.806	0.006	**1.763**	**1.702**	**0.027**	141.0	1.1
930 A/6 42-45 cm	**39/1**	**43.5±1.5**	2.995	±0.005	0.2519	±0.0006	817.7	±0.21	0.02233	±0.80	1.1441	±0.15	0.0010	2.175	0.007	**2.149**	**2.088**	**0.018**	145.0	1.5
930 B/6 107-110 cm	**39/3**	**108.5±1.5**	3.228	±0.004	0.3177	±0.0007	898.7	±0.18	0.02874	±0.73	1.1439	±0.13	0.0013	2.804	0.009	**2.774**	**2.713**	**0.021**	145.0	1.3
930 B/6 134-137 cm	**35/9**	**135.5±1.5**	3.017	±0.003	0.3137	±0.0006	878.8	±0.21	0.02970	±0.73	1.1394	±0.11	0.0017	2.911	0.008	**2.878**	**2.817**	**0.022**	140.6	1.1
930 B/6 134-137 cm	**39/10**	**135.5±1.5**	3.019	±0.003	0.2414	±0.0008	1149.4	±0.41	0.02995	±0.65	1.1441	±0.11	0.0011	2.916	0.012	**2.891**	**2.830**	**0.019**	145.3	1.1
930 B/6 142-146 cm	**36/1**	**144.0±2.0**	2.804	±0.003	0.1327	±0.0002	1874.3	±0.15	0.02900	±0.40	1.1431	±0.11	0.0007	2.816	0.008	**2.801**	**2.740**	**0.012**	144.3	1.1
930 B/6 142-146 cm	**40/2**	**144.0±2.0**	2.823	±0.003	0.1503	±0.0006	1681.9	±0.42	0.02926	±0.55	1.1432	±0.12	0.0006	2.843	0.012	**2.826**	**2.765**	**0.016**	144.4	1.2
930 C/6 251-254 cm	**38/9**	**252.5±1.5**	3.024	±0.004	0.0999	±0.0002	2962.0	±0.27	0.03205	±0.34	1.1425	±0.12	0.0003	3.112	0.009	**3.101**	**3.040**	**0.011**	143.7	1.2
930 D/6 312-314 cm	**36/2**	**313.0±1.0**	2.746	±0.003	0.3625	±0.0006	772.6	±0.14	0.03310	±0.82	1.1414	±0.11	0.0023	3.249	0.009	**3.208**	**3.147**	**0.027**	142.6	1.1
930 D/6 356-358 cm	**39/7**	**357.0±1.0**	3.036	±0.004	0.2515	±0.0005	1256.8	±0.16	0.03394	±0.54	1.1441	±0.12	0.0012	3.308	0.009	**3.282**	**3.221**	**0.018**	145.5	1.2
930 E/6 438-440 cm	**36/6**	**439.0±1.0**	2.780	±0.003	0.2672	±0.0004	1180.8	±0.13	0.03699	±0.56	1.1391	±0.11	0.0016	3.628	0.010	**3.598**	**3.537**	**0.021**	140.5	1.1
HWU20110609/002A	**67/1**	**seafloor**	3.081	±0.004	0.1179	±0.0002	1064.6	±0.21	0.01326	±0.63	1.1453	±0.12	0.0002	1.282	0.004	**1.270**	**1.207**	**0.008**	145.8	1.2
1151	**67/2**	**seafloor**	2.891	±0.004	0.1576	±0.0002	810.7	±0.20	0.01435	±0.81	1.1450	±0.14	0.0003	1.392	0.005	**1.375**	**1.312**	**0.011**	145.5	1.5
56-08/928	**67/3**	**seafloor**	2.888	±0.004	0.1715	±0.0003	1458.5	±0.19	0.02827	±0.49	1.1434	±0.13	0.0003	2.747	0.008	**2.729**	**2.666**	**0.014**	144.5	1.3
D340B/1496a	**67/4**	**seafloor**	3.553	±0.005	0.1458	±0.0002	979.6	±0.21	0.01308	±0.69	1.1451	±0.13	0.0002	1.265	0.004	**1.252**	**1.189**	**0.009**	145.6	1.3
1157 A	**78/27**	**seafloor**	2.528	±0.003	0.1611	±0.0002	68.6	±0.91	0.00123	±10.47	1.1462	±0.11	0.0005	0.137	0.001	**0.117**	**0.054**	**0.012**	146.3	1.1
1157 B	**78/28**	**seafloor**	2.628	±0.003	0.1449	±0.0002	82.1	±0.80	0.00131	±8.50	1.1454	±0.11	0.0004	0.142	0.001	**0.124**	**0.061**	**0.011**	145.4	1.1
20110707/008A	**78/30**	**seafloor**	2.866	±0.003	0.1532	±0.0002	1069.3	±0.24	0.01861	±0.64	1.1453	±0.11	0.0003	1.802	0.006	**1.785**	**1.722**	**0.012**	146.0	1.2
20110608/012A	**78/31**	**seafloor**	3.152	±0.003	0.2101	±0.0003	716.0	±0.31	0.01547	±0.93	1.1452	±0.11	0.0004	1.503	0.006	**1.482**	**1.419**	**0.014**	145.8	1.1
[*]**930 D/6 377-379 cm**	**36/3**	**378.0±1.0**	2.304	±0.002	0.3012	±0.0005	855.4	±0.13	0.03633	±0.74	1.1426	±0.11	0.0023	3.562	0.009	**3.522**	**3.461**	**0.027**	144.0	1.1
[*]**930 D/6 377-379 cm**	**40/3**	**378.0±1.0**	3.801	±0.004	0.2619	±0.0009	965.1	±0.36	0.02163	±0.75	1.1423	±0.12	0.0010	2.106	0.009	**2.084**	**2.023**	**0.016**	143.2	1.2
[*]**930 D/6 388-392 cm**	**24/8**	**390.0±2.0**	2.761	±0.003	0.2425	±0.0005	1237.3	±0.19	0.03543	±0.55	1.1426	±0.12	0.0012	3.460	0.010	**3.432**	**3.371**	**0.020**	144.0	1.3
[*]**930 D/6 388-392 cm**	**40/4**	**390.0±2.0**	3.232	±0.004	0.3715	±0.0013	879.5	±0.35	0.03285	±0.79	1.1423	±0.12	0.0017	3.216	0.014	**3.180**	**3.119**	**0.026**	143.6	1.2

[a]Location of the coral fragments within the cores ± half of their length.

[b-c] Calculated ages before and after correction for ^{230}Th, respectively. The ages are in years before 2014.

[*]Downcore sampes out of stratigraphic sequence and presenting two distinct U-series ages, the corresponding radiocarbon analyses for these samples were not considered in this study.

Table 3

		U-series ages			Radiocarbon ages				Calculated data			
Sample Name	[a]Depth (cm)	Lab number	Date corr (yrs BP_{1950})	±1s (abs)	Lab number	$\delta^{13}C_{VPDB}$± 0.1 (‰)	Conventional ^{14}C-age (yrs BP)	±1s	Δ14C (‰)	±1s (abs)	MRE (yrs)	±1s (abs)
1157 A	**seafloor**	78/27	**54**	**6**	SUERC-33524	-6.7	**404**	**35**	**-43**	**4**	**321**	**36**
1157 B	**seafloor**	78/28	**61**	**5**	SUERC-33524	-6.7	**404**	**35**	**-42**	**4**	**309**	**36**
D340B/1496a	**seafloor**	67/4	**1189**	**4**	SUERC-36977	-4.7	**1742**	**36**	**-70**	**4**	**464**	**38**
HWU20110609/002A	**seafloor**	67/1	**1207**	**4**	SUERC-36969	-5.3	**1827**	**35**	**-78**	**4**	**561**	**37**
1151	**seafloor**	67/2	**1312**	**6**	SUERC-33519	-5.1	**1821**	**35**	**-66**	**4**	**394**	**38**
20110608/012A	**seafloor**	78/31	**1419**	**7**	SUERC-36968	-6.9	**1989**	**35**	**-73**	**4**	**418**	**40**
930 A/6 4-6 cm	**5.0±1.0**	35/8	**1702**	**13**	SUERC-33528	-5.4	**2283**	**37**	**-75**	**5**	**513**	**46**
20110707/008A	**seafloor**	78/30	**1722**	**6**	SUERC-36973	-5.9	**2211**	**35**	**-65**	**4**	**400**	**38**
930 A/6 42-45 cm	**43.5±1.5**	39/1	**2088**	**9**	SUERC-39973	-7.7	**2467**	**37**	**-53**	**4**	**367**	**39**
56-08/928	**seafloor**	67/3	**2666**	**7**	SUERC-36975	-5.1	**2835**	**35**	**-30**	**4**	**379**	**36**
930 B/6 107-110 cm	**108.5±1.5**	39/3	**2713**	**10**	SUERC-39974	-6.0	**2885**	**35**	**-31**	**4**	**368**	**41**
930 B/6 142-146 cm	**144.0±2.0**	36/1	**2740**	**6**	SUERC-36956	-5.8	**2894**	**35**	**-28**	**4**	**321**	**42**
930 B/6 142-146 cm	**144.0±2.0**	40/2	**2765**	**8**	SUERC-36956	-5.8	**2894**	**35**	**-25**	**4**	**222**	**41**
930 B/6 134-137 cm	**135.5±1.5**	39/10	**2830**	**10**	SUERC-36955	-6.5	**2937**	**35**	**-23**	**4**	**207**	**38**
930 B/6 134-137 cm	**135.5±1.5**	35/9	**2817**	**11**	SUERC-36955	-6.5	**2937**	**35**	**-24**	**4**	**205**	**37**
930 C/6 251-254 cm	**252.5±1.5**	38/9	**3040**	**6**	SUERC-36957	-7.8	**3232**	**35**	**-34**	**4**	**329**	**37**
930 D/6 312-314 cm	**313.0±1.0**	36/2	**3147**	**13**	SUERC-36958	-7.2	**3367**	**35**	**-38**	**4**	**407**	**39**
930 D/6 356-358 cm	**357.0±1.0**	39/7	**3221**	**9**	SUERC-37504	-6.8	**3447**	**37**	**-39**	**5**	**417**	**39**
929 A/4 3-9 cm	**6.0±3.0**	36/8	**3367**	**9**	SUERC-33527	-5.2	**3728**	**35**	**-55**	**4**	**592**	**41**
929 A/4 12-17 cm	**14.5±2.5**	24/1	**3530**	**8**	SUERC-36945	-5.0	**3706**	**35**	**-34**	**4**	**414**	**36**
930 E/6 438-440 cm	**439.0±1.0**	36/6	**3537**	**10**	SUERC-36964	-6.9	**3664**	**35**	**-28**	**4**	**377**	**37**
929 B/4 106-108 cm	**107.0±1.0**	36/9	**3716**	**10**	SUERC-36947	-4.8	**3825**	**35**	**-26**	**4**	**351**	**39**
929 A/4 90-91cm	**90.5±0.5**	39/9	**3765**	**7**	SUERC-36946	-4.4	**3850**	**35**	**-24**	**4**	**354**	**37**
929 B/4 188-189 cm	**188.5±0.5**	35/3	**3986**	**9**	SUERC-36948	-5.9	**4015**	**35**	**-17**	**4**	**337**	**41**
929 D/4 310-312 cm	**311.0±1.0**	36/10	**4207**	**12**	SUERC-36952	-5.0	**4156**	**35**	**-8**	**5**	**348**	**38**
929 C/4 284-290 cm	**287.0±3.0**	35/1	**4216**	**8**	SUERC-36949	-6.5	**4115**	**35**	**-2**	**4**	**313**	**37**
929 D/4 349-353 cm	**351.0±2.0**	35/6	**4256**	**12**	SUERC-36953	-5.9	**4151**	**35**	**-2**	**5**	**292**	**38**

[a]Location of the coral fragments within the cores ± half of their length.